inventions

Article

The Potential of Lakes for Extracting Renewable Energy—A Case Study of Brates Lake in the South-East of Europe

Eugen Rusu [1], Puiu Lucian Georgescu [2], Florin Onea [1,*], Victoria Yildirir [1] and Silvia Dragan [3]

[1] Department of Mechanical Engineering, Faculty of Engineering, "Dunarea de Jos" University of Galati, 800008 Galati, Romania; eugen.rusu@ugal.ro (E.R.); victoria.caranfil@ugal.ro (V.Y.)
[2] Department of Chemistry, Physics and Environment, REXDAN Research Infrastructure, "Dunarea de Jos" University of Galati, 800008 Galati, Romania; lucian.georgescu@ugal.ro
[3] EnviroEcoSmart, Str. Nufarului, nr. 3, 800298 Galati, Romania; silvia.dragan@gmail.com
* Correspondence: florin.onea@ugal.ro

Abstract: The aim of this work is to provide some details regarding the energy potential of the local wind and solar resources near the Galati area (south-east of Romania) by considering the performances of a few recent technologies. Based on 22 years of ERA5 data (2001–2022), a picture concerning the renewable energy resources in the Brates Lake area is provided. Comparing the wind and solar resources with in situ and satellite data, a relatively good agreement was found, especially in regards to the average values. In terms of wind speed conditions at a hub height of 100 m, we can expect a maximum value of 19.28 m/s during the winter time, while for the solar irradiance the energy level can reach up to 932 W/m^2 during the summer season. Several generators of 2 MW were considered for evaluation, for which a state-of-the-art system of 6.2 MW was also added. The expected capacity factor of the turbines is in the range of (11.71–21.23)%, with better performances being expected from the Gamesa G90 generator. As a next step, several floating solar units were considered in order to simulate large-scale solar projects that may cover between 10 and 40% of the Brates Lake surface. The amount of the evaporated water saved by these solar panels was also considered, being estimated that the water demand of at least 3.42 km^2 of the agricultural areas can be covered on an annual scale.

Keywords: Romania; Brates Lake; floating solar; wind turbine; ERA5; evaporation

Citation: Rusu, E.; Georgescu, P.L.; Onea, F.; Yildirir, V.; Dragan, S. The Potential of Lakes for Extracting Renewable Energy—A Case Study of Brates Lake in the South-East of Europe. *Inventions* **2023**, *8*, 143. https://doi.org/10.3390/inventions8060143

Academic Editors: Theocharis Tsoutsos and Tek-Tjing Lie

Received: 16 October 2023
Revised: 3 November 2023
Accepted: 7 November 2023
Published: 9 November 2023

1. Introduction

The aim of the European Green Deal published in 2019 is to promote the use of renewable energy (RE) sources in order to obtain a significant reduction in the carbon footprint. To achieve such ambitious targets, the expected milestones involve a CO_2 decrease by 55% in 2030 (compared to 1990), reaching zero emissions by 2050. For the first time, in 2020, the energy generated from RE sources in Europe exceeded the fossil fuel production, which is mainly supported by the wind and hydropower sector. In addition, it is worth mentioning that solar technologies are considered to be the most dynamic RE market in this region, including the development of the floating photovoltaic (FPV) projects [1]. Over the last years, the evolution of the wind sector involved various paths, with some studies suggesting that the North Sea could become the next hot spot in terms of electricity production [2]. At the end of 2022, the European Union (EU-27) was defined by an installed capacity of 204 GW, of which 92% was located onshore. From the total electricity mix, the wind contribution is more visible in the case of Denmark with 55%, being followed by Germany, Portugal, Spain, and Sweden with percentages close to 25%. The expected capacity factor of the new onshore wind projects reach up to 45% in relation to a generator of 4.1 MW (average value), compared to the offshore ones where a 50% capacity factor and an average power of 8.0 MW are noticed [3]. The European solar industry registered an impressive growth of 50% per year during the interval 2006–2016, decreasing to a rate of

32% in 2017. Nevertheless, at this moment, the solar market seems to be in a saturation stage, which indicates that if the investment level does not increase, this RE source will have a limited influence on the energy mix in the time interval 2030–2040 [4]. However, considering the recent technology developments, some new opportunities occurred such as the development of the FPV projects that can be installed on different water bodies of Europe, similar to the ones from the coastal areas, hydropower reservoirs, and even urban lakes [5]. An FPV has the potential to reduce the algae growth and water evaporation, has better performance than an onshore farm due to lower water temperature, and will not compete with the land use, while the shading effect will be minimal [6,7]. At the end of 2018, almost 1.3 GWp of FPV were installed on a global scale, compared to almost 500 GWp accounted by the onshore market [8].

As it is located in the northern hemisphere, Romania is one of the largest countries from the south-eastern part of Europe, covering a surface of 240,000 km^2. The combination between the geographical and climatic features makes this area a suitable candidate for the development of renewable projects, such as solar projects [9,10]. It is estimated that the average sunshine period varies between 1600 and 3200 h/year, with more important photovoltaic projects being developed in the low relief areas, such as the Moldavian and Dobrogea Plateaus in the east. During the interval 2007–2013, a total of EUR 350.556 million was allocated to the Romanian renewable sector, while after 2010 a total of 305 photovoltaic projects (1351 MW) were developed in areas that cover a total of 3000 ha. For the interval 2010–2019, the investments in the solar sector covered almost EUR 2000 million, from which a maximum peak was associated with the interval 2012–2014, where almost 90% of this budget was allocated. The investment level significantly dropped at the end of 2019, of which only 2.5 MW of solar systems are implemented, compared to a peak value of 863.43 MW indicated for the year 2013 [11]. At this point, we have to mention that there are no FPV projects operating in this region, although at one moment, some plans to develop a combined offshore wind and floating solar project were vehiculated [12]. Except for the mountain areas, the most important Romanian regions for the development of wind projects can be also found in the eastern part, more precisely near the Black Sea, Danube Delta, Northern Dobrogea, or even the Barlad Plateau, where the annual wind speed can reach up to 10 m/s (50 m in height). As a consequence, a significant part of the operational wind farms is located in these areas, which is indicated by a share of 78% for Dobrogea and the southern part of the Barlad Plateau, including the Galati/Braila counties [13]. Definitely, the project Fantanele–Cogealac (600 MW) is one of the most representative Romanian wind farms, being defined by a total of 240 generators that operate at a hub height of 100 m. A total of EUR 1.1 billion was allocated to this project, which is expected to cover a share of 10% of the total Romanian RE production [14].

Galati County is located in the eastern part of Romania, being a major port at the Danube River [15]. Although several renewable projects (for example, wind and solar) are operational in this area, there is little information about the local energy potential that is disseminated from an academic perspective. Thus, there is still room for development, which in fact, is shown by the approval of a 629 MW wind project run by the Hoopeks International Company. This will involve a total of 136 generators (of 6.2 MW), an investment cost of EUR 500 million, and a covered area of 13,000 ha. More than these two photovoltaic project requests (of 310 MW each) were approved for development in the middle of 2022 [16]. In addition, we need to mention that Liberty Galati, which is the largest steel factory in Romania, is aiming to reduce the CO_2 fingerprint by almost 80% using the RE sources. More precisely, there is an increased interest to reduce electricity consumption by developing a capacity of 20 MW wind farm and 180 MW solar farm on site, which may be also used for the production of green hydrogen [17]. This strategy is clearly in line with the current EU regulations, targeting the CO_2 emissions, which in general, are higher in the eastern part of Europe [18].

In conclusion, for the first time, a lake environment from Romania is evaluated from the point of view of a source of renewable energy. This may lead to further applications, such as the implementation of an FPV pilot project on the Brates Lake. This approach represents a step forward in the sustainable development of this area, where multiple projects can be developed in order to support recreational activities or the local aquaculture industry.

The present work is structured as follows. After the Introduction, in Section 2, all the information regarding the target area and numerical datasets are provided, including the mathematical approach used to assess the performance of renewable systems. Then, in Section 3, the renewable profile of the Brates Lake area is assessed by taking into account various meteorological parameters, including the expected benefits resulting from the implementation of different FPV scenarios. Finally, in Section 4, the importance of the Galati County from a renewable project point of view is highlighted, including some key findings of the present work.

2. Materials and Methods

2.1. Study Area

The target area is located in the eastern part of Romania, more precisely, north of Galati City [19], as illustrated in Figure 1. During the 18th and 19th centuries, this lake had a surface of about 100 km^2, while at this moment, the lake has been drained due to various human interventions, being reduced to a surface of 20 km^2 and a maximum water depth of 3 m [20]. At this point, we should also mention that the Brates Lake is in a higher degradation state and the inefficiency of the water processing plants operating in this area is indicated as a main factor for this degradation [21]. At one point, this lake was connected to the Danube and Prut Rivers [22], throughout different channels, being frequently used for fisheries, and more recently, for agricultural purposes [23]. In total, the Brates Lake ecosystem health is uncertain since there are no monitoring stations or projects focused on this area, while significantly more attention is being given to the Danube River [24–26].

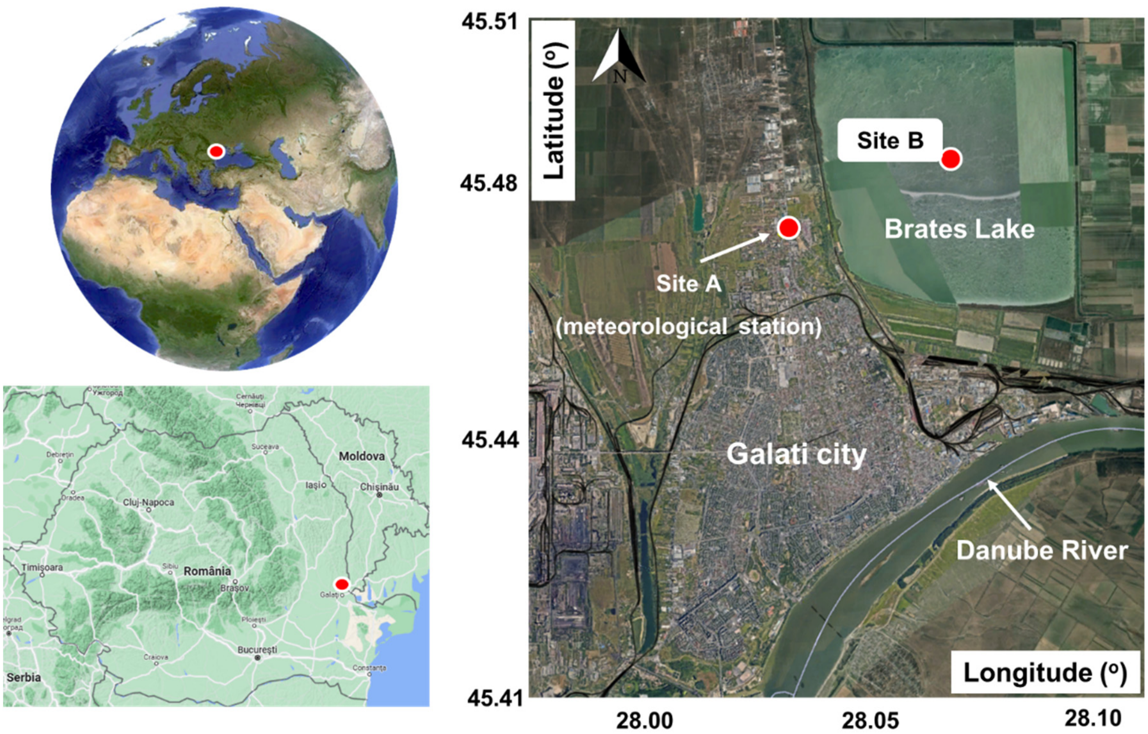

Figure 1. Overview of the targeted area, including the location of site A (the meteorological station) and site B (in the middle of Brates Lake). Information is processed from Google Earth 2023.

In this area, two specific sites denoted as A and B are considered for analysis. Site A corresponds also to the position of a meteorological station maintained by the National Meteorological Administration of Romania (or NMA-RO), with the associated wind measurements ($U10$) being used to check the accuracy of the reanalysis data. Site B (Brates

Lake) will be further considered to highlight the profiles of the renewable resources (wind and solar), and the performances of some onshore wind turbines and floating solar panels.

2.2. Wind and Solar Datasets

Several datasets and variables were considered in the present work, as presented in Table 1. In situ wind measurements are available only for site A, being associated with a reference height of 10 m ($U10$). Twenty-two years of data (January 2001–December 2022) were processed, with the time series involving daily values of the average and maximum wind speed values. For the same time interval, the ERA5 wind dataset was considered for comparison, including the hourly values (24 values per day) and u and v components. The ERA5 dataset is a project associated with the European Centre for Medium-Range Weather Forecasts (ECMWF) that has a spatial resolution of 30 km, being frequently used by researchers to identify the renewable energy potential from various geographical environments [27–29]. From a meteorological point of view, the $U10$ parameter is more relevant [30], but for a wind turbine, it is more important to consider the wind conditions that are characteristic at the hub height level (for example, 100 m) [31,32].

Table 1. The main characteristics of the reference sites considered in the present work. Information is processed from Google Earth 2023.

Location	ID	Data Type	Parameter	Latitude (°)	Longitude (°)
Galati	Site A	In situ, ERA5	$U10$	45.473	28.032
Galati	Site B	ERA5, SARAH	$U100$, $SSRD$, Temp, Evaporation	45.483	28.070

One way to identify the solar energy potential involves the use of the surface solar radiation downwards ($SSRD$ in J/m^2), that was processed from the ERA5 package (24 values per day), which is defined as a combination of direct and diffuse solar radiation that reached a horizontal plane from the Earth. By dividing this parameter with the accumulation period (3600 s), a new form that is expressed in W/m^2 can be obtained [33]:

$$\text{Solar irradiance} = \frac{SSRD}{3600} \tag{1}$$

In addition, the daily temperature (temperature at 2 m height) and evaporation rate from the ERA5 database, were considered and processed, in order to provide a more complete picture of the local environmental conditions (daily values for the interval 2001–2022). The presence of an FPV project can significantly reduce the volume of the evaporated water [34–36]; therefore, another objective of this work is to estimate the water prevention for the Brates Lake area.

The in situ measurements used in this work are available only for the wind conditions, and as a consequence, the SARAH data record [37,38] will be used to check the accuracy of some other parameters (for example, temperature and solar irradiance). These data are available on the PVGIS website (https://re.jrc.ec.europa.eu/pvg_tools/en/#api_5.1, accessed on 7 March 2023), which is associated with site B (Brates Lake) for the interval January 2005–December 2016.

2.3. Wind and Solar Systems

In Table 2 and Figure 2, the main features of the onshore turbines considered for evaluation are presented. These systems are defined by a rated power of 2 MW, except for the general electric turbine (2.5 MW), with similar generators operating in the wind projects from this region.

Table 2. Technical characteristics of the selected onshore wind turbines [39–41].

Turbine	Rated Power (MW)	Cut-In Speed (m/s)	Rated Speed (m/s)	Cut-Out Speed (m/s)	Hub Height (m)
General Electric 2.5xl (T1)	2.5	3.5	13.5	25	75/100
Vestas V90-2.0 (T2)	2	4	13	25	80/95/105
Enercon E82-E2 (T3)	2	2	12.5	25	78/85/98/108/138
Gamesa G90 (T4)	2	3	11	21	67/78/90/100
Vestas V162-6.2 MW	6.2	3	N/A	25	119/125/166/169

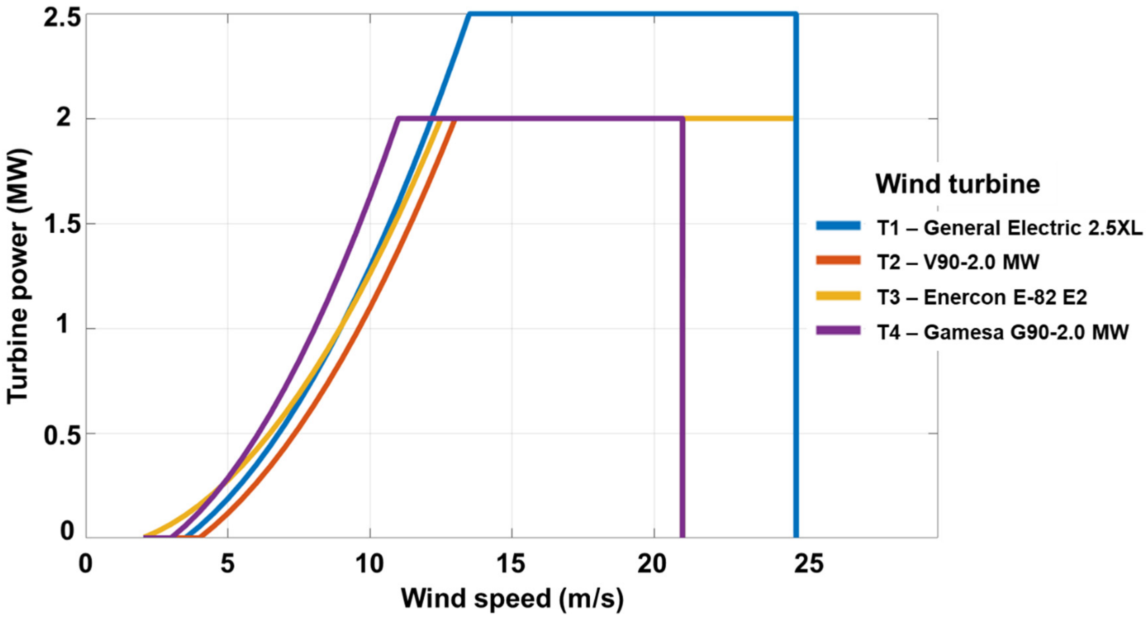

Figure 2. Power curves representation of the considered onshore wind turbines.

By looking at the future onshore wind farms expected to be implemented in this area, we may notice that this will include higher capacity systems that can reach up to 6.2 MW per turbine (www.zf.ro, accessed on 20 April 2023). Moreover, by looking at the wind turbine market, it is possible that this will involve a Vestas V162-6.2 MW system, which will be installed in some other regions from Romania. According to the technical details provided by the Vestas Company for this turbine, the cut-in value is set at 3 m/s, while the cut-out value is similar to the other generators (25 m/s). Nevertheless, the rated wind speed is not provided, which means that this will be further identified in comparison with similar wind generators (for example, Senvion 6.2M152).

Although the profile of the 2 MW turbines may appear to look similar, the main differences occur in terms of the cut-in and rated wind speed values, with the most performant from this point of view being turbines T3 and T4. In addition, the hub height of each system can be adjusted, with values ranging from 67 m (T4) to a maximum of 138 m (T3). Corresponding to this particular height, the performance of each turbine will be adjusted by changing the $U100$ parameter to the value for a particular level, as follows [42]:

$$U_{hub} = U_{100} \cdot \ln\left(\frac{z_{hub}}{z_0}\right) / \ln\left(\frac{z_{100}}{z_0}\right) \tag{2}$$

where U_{hub} is the wind speed associated with a particular hub height, z_{hub} and z_{100} are the reference heights (turbine and 100 m), and z_0 is the roughness factor computed for site B (water surface = 0.0002 m).

The annual electricity production (or AEP) of a wind turbine can be estimated as [43] follows:

$$AEP = 8760 \cdot \int_{cut\text{-}in}^{cut\text{-}out} P(u)f(u)du \tag{3}$$

where 8760 is the number of hours per year, $P(u)$ is the wind turbine power curve, *cut-out/cut-in* are the turbine operational limits. As for the Weibull probability density function or $f(u)$, this can be defined as follows [43]:

$$f(u) = \left(\frac{k}{c}\right)\left(\frac{u}{c}\right)^{k-1} \exp\left[-\left(\frac{u}{c}\right)^{k}\right] \tag{4}$$

where u is the wind speed and k, c are the shape and scale parameters.

Since the Galati area presents suitable solar resources for the development of renewable projects, another objective of the present work is to identify how a floating solar farm may perform for the Brates Lake area. In total, this may be considered as an element of novelty, taking into account that there is not yet a similar project in Romania. In Table 3, the characteristics of the floating modules considered are presented.

Table 3. Specification of the floating solar PV modules [44–47].

Parameter	Q-Power-G5 280 (P1)	GCLM6/60H-325 (P2)	Trina Solar (P3)	JRH 540 W (P4)
Power (W)	280	325	375	540
Efficiency (%)	17.10	20.00	19.30	21.35
Surface (m^2)	1.94	1.62	1.95	2.58

We can notice that the power varies from 280 to 540 W, while the maximum efficiency (21.35%) and surface panel (2.58 m^2) are associated with the JRH 540 W system.

Based on these characteristics, the expected power output of a solar panel can be simply estimated as follows [33]:

$$AEP_{solar} = Irradiance \cdot A_s \cdot T_{irradiance} \cdot \eta \tag{5}$$

where *irradiance* is solar irradiance (in W/m^2), A_s is the solar panel area, $T_{irradiance}$ denotes the hours of solar irradiance, and η is the solar panel efficiency.

Besides the electricity output, another advantage of an FPV project is that it can save the amount of evaporated water by blocking sunlight. For the present work, several scenarios (10, 20, 30, and 40%) were considered, where various percentages of the lake surface (20 km^2 in total) were covered by solar panels. A 40% scenario can be considered to be a realistic one, taking into account that there are studies where a 50% scenario was associated with a lake area of 100 km^2, this being the case of Walker Lake [35]. Table 4 presents the expected installed capacity (in MW) for each scenario, where the water surface associated with each scenario was divided by the area covered by the total number of solar panels. The number of panels and the capacity rapidly increase as we move to the 40% scenario in a realistic way, with a 10% scenario being easier to implement in a short-term period.

A similar approach (as presented in [48]) will be used to quantify the volume of the evaporated water associated with the presence of an FPV project for the Brates Lake area. First, the natural evaporation of the lake (no FPV) is estimated as follows:

$$V(\mathrm{m}^3/\mathrm{day}) = E(\mathrm{m}/\mathrm{day}) \times A_{Lake}(\mathrm{m}^2) \tag{6}$$

while the amount of water saved by the presence of the FPV is indicated as follows:

$$\Delta V(\mathrm{m}^3/\mathrm{day}) = k \times E(\mathrm{m}/\mathrm{day}) \times A_{CA}(\mathrm{m}^2) \tag{7}$$

where E is the amount of evaporation (from ERA5), A_{Lake} is the Brates Lake area (20 km^2), k is the reduction factor associated with the type and FPV platform (k = 0.6), and A_{CA} is the area covered by the FPV panels.

Table 4. Scenarios involving the Brates Lake area and the considered FPV systems. The installed capacity required for each solar project is indicated in MW.

FPV System	**Brates Lake—Scenarios**			
	10% (2 km^2)	**20% (4 km^2)**	**30% (6 km^2)**	**40% (8 km^2)**
Q-Power-G5 280	289	577	866	1155
GCLM6/60H-325	401	802	1204	1605
Trina Solar	385	769	1154	1538
JRH 540 W	418	836	1254	1672

3. Results and Discussion

A first perspective of the Romanian electricity market is provided in Figure 3 by processing the data provided through the national authorities (https://www.sistemulenergetic.ro/, accessed on 20 April 2023) for the interval January 2008–December 2022. It is important to mention that each value is indicated in MW, which is related to the electricity delivered to the system for a particular time frame (for example, 30 March 2023 h 10:39:05). In terms of production/consumption (Figure 3a), we can notice that for the time period 2008–2017, electricity production was more significant, reaching a maximum of 9243 MW. After this interval, the market started to equalize, with the intervals being more visible when the consumption was more dominant. This is a possible explanation for the occurrence of a dry summer season that limits the performance of the Iron Gate hydroelectric power station. The electricity import/export evolution is provided in Figure 3b, considering only the time interval (2020–2022). The exports are significantly lower (56%) than the imports and the maximum peaks are below 2400 MW, with an average value of 537 MW being expected in general. For the imports, the average value is about 652 MW, while peaks of 2600 MW are frequently noticed. The evolution of the wind and photovoltaic sector is provided in Figure 3c, with more significant contributions being noticed from the wind projects. Starting in 2010, the wind market became more visible, being influenced by the presence of the winter season (more energetic) during which maximum peaks of 2000 MW can be delivered to the national electricity network. The contribution of the solar sector is smaller, being estimated that during the interval 2013–2022, on a sunny day during the peak periods, almost 879 MW were generated. In Figure 3d, a normalized plot is designed (instant value/maximum value) including the consumption and wind/solar contribution, considering only the interval 2020–2022. The electricity consumption in Romania starts to increase around 8:00 AM, after which the values remain constant until 09:00 PM. As expected, the solar sector reaches peak performance during the day time (around 12:00), compared to the wind sector where the best performances are expected during the night time (starting at 09:00 PM). This calculation includes all the electricity consumers, and therefore it is difficult to identify the behavior of the industrial and residential sector.

An overview of the main parameters related to the Brates Lake area is provided in Figure 4, where the monthly boxplots of ERA5 data cover a time interval of 22 years (2001–2022). The seasonal differences between the summer and winter seasons are visible, indicating various patterns according to the characteristic taken into account. For example, in the case of the U100 conditions (Figure 4a), higher values are expected during January, where an extreme wind speed value of 19.28 m/s may occur, compared to only 13.28 m/s expected in December. The median values range from 4.28 m/s (July) to a peak of 5.80 m/s in March. The solar irradiance is very low during the interval September–April with median values below 41.02 W/m^2, gradually increasing to 124.30 W/m^2 in July. No outliers are visible for the interval April–September, compared to the winter season. A maximum peak of 932.90 W/m^2 is expected in June, gradually decreasing to a value of 148.53 W/m^2 in December, in the case of the 95 percentile.

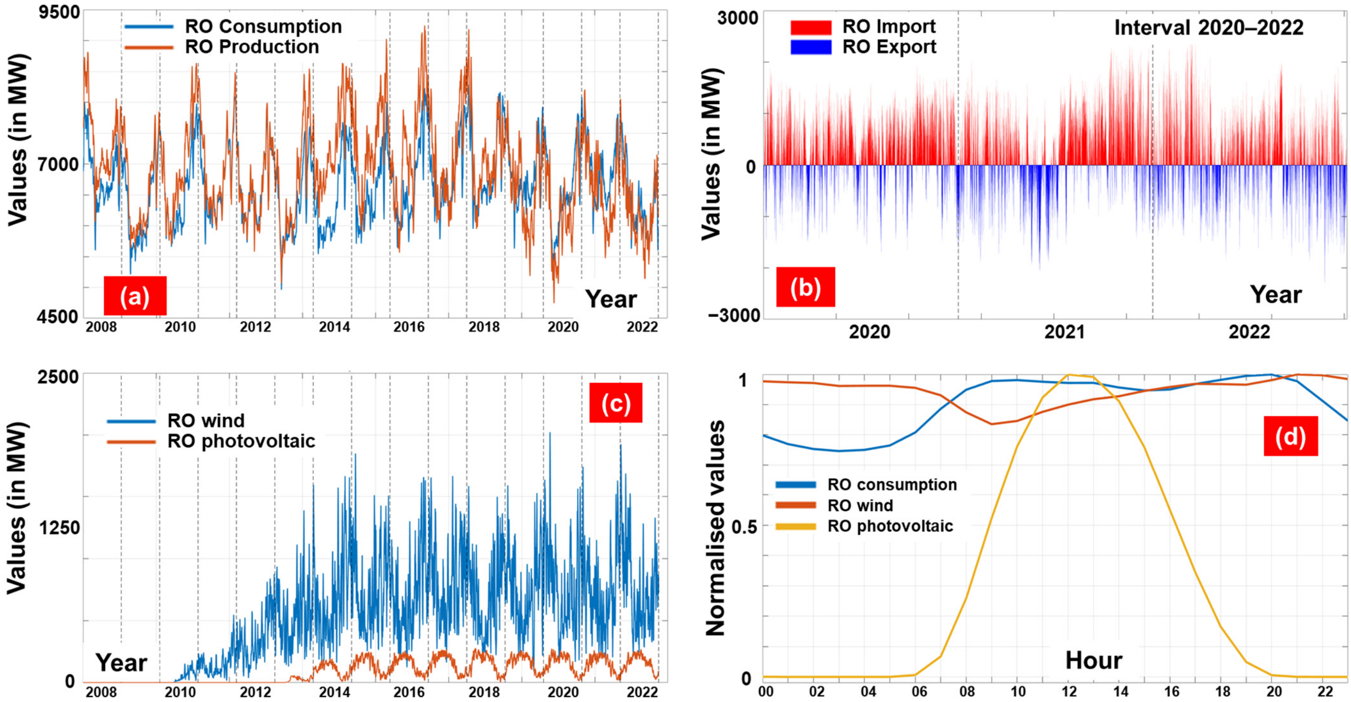

Figure 3. The Romanian national electricity balance represented for (**a**) consumption/production averaged time series for the interval 2008–2022; (**b**) import/export averaged time series during the interval 2020–2022; (**c**) evolution of the wind/PV market for the interval 2008–2022; (**d**) hourly normalized values of the consumption and wind/PV sector expected during 2020 and 2022.

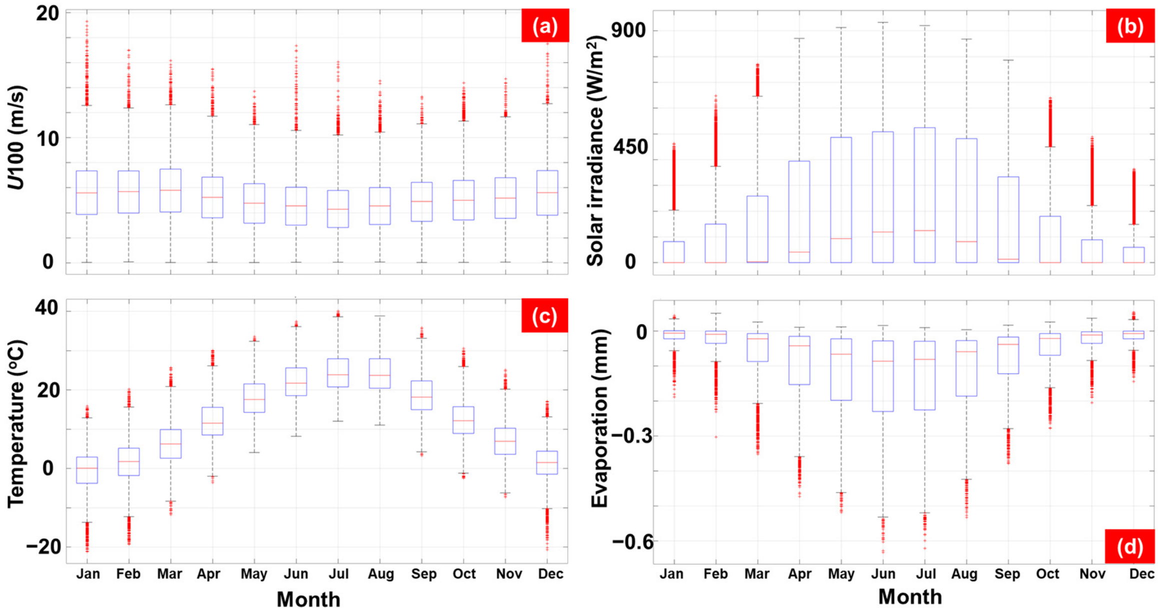

Figure 4. Monthly distribution of the main physical parameters related to the Brates Lake (site B). Boxplots based on the ERA5 data (2001–2022), where (**a**) *U*100 in m/s; (**b**) solar irradiance in W/m^2; (**c**) temperature in °C; (**d**) evaporation (mm of water equivalent—negative values).

In the case of the temperature (Figure 4c), the values oscillate between −21.14 °C and 40 °C, with median values of 0 °C being expected in January, 33.59 °C in May, and 12.17 °C in October, respectively. The evaporation rate (per day) is illustrated in Figure 4d, being estimated in terms of mm of water equivalent, where the positive values indicate condensation. During June and July, the evaporation rate is much higher, reaching a maximum value of 0.53 mm, compared to 0.14 mm in December. As it can be noticed, the condensation presents smaller values, with a more important contribution being expected during the interval January–February.

The ERA5 project represents the main source of data for the present work, and as a consequence, the accuracy of these values needs to be checked. As a first step, Figure 5 provides a first analysis of the ERA5 data, where the monthly wind measurements from site A (*U*10) are compared with the ones from the meteorological station that operates in this location. As it can be noticed, ERA5 overestimates the average wind speed, while a reverse pattern is expected in the case of the maximum values. For example, ERA5 presents average values in the range of [2.73–3.36] m/s and maximum values that reach between [8.93 and 12.31] m/s. The meteorological data indicate average values of [2.31–3.13] m/s, while the maximum can reach up to 28 m/s. The in situ maximum values are defined by a random variation, with extreme values being possible during the summer season. This aspect is not visible in the case of the ERA5 data, where the maximum values are defined by a smooth monthly fluctuation. This is a characteristic of the reanalysis dataset, where the values are averaged over a particular grid box [49].

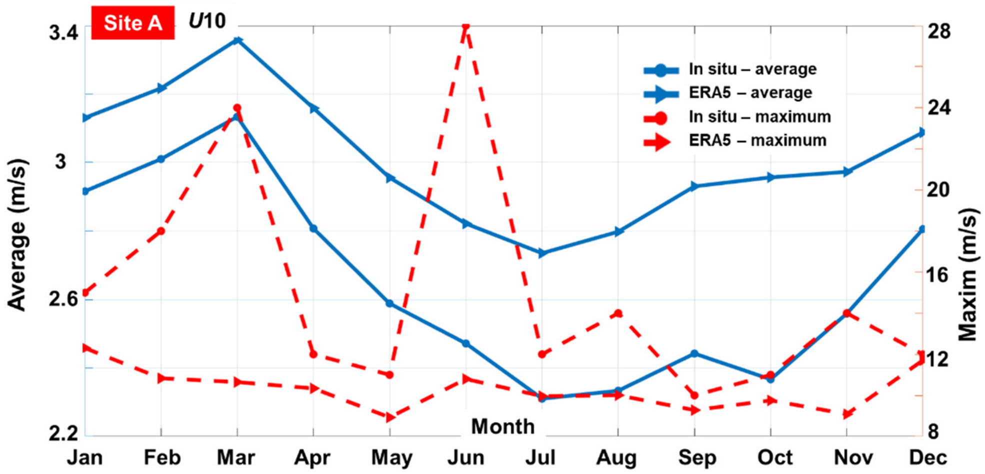

Figure 5. *U*10—direct comparison between in situ and ERA5 data for the time interval 2001–2020, where the left axis denotes average values and the right axis denotes maximum values.

Figure 6 provides the monthly evaluation for the solar irradiance and temperature parameters by making a direct comparison between ERA5 and SARAH data for the interval 2005–2016.

In terms of the solar values (Figure 6a), ERA5 seems to overestimate this parameter, indicating a maximum of 267.2 W/m^2 during June/July compared to only 209.5 W/m^2, which is expected from the SARAH data for the same time interval. Depending on the month taken into account, the differences between the two datasets are in the range of [21.5–31]%, with higher values being expected during the winter time. A different pattern is noticed for the temperature data (Figure 6b), where a good agreement is noticed between the mentioned datasets.

A more detailed analysis of the *U*100 parameter is provided in Figure 7, considering that at this time, the wind roses are associated with each season. According to this information, the north and south sectors correspond to the dominant wind direction, with the northern sector being defined by more energetic wind resources that frequently exceed 8 m/s. Each season is defined by particular features that, for example, in the case of the summer time, will indicate a concentration of the wind from the northern part, which will reach almost 10% from the entire dataset. As we move to the winter period, it is possible to notice a significant presence of the wind action from the south-west sector that will have an impact on the performance of a particular wind project. The spring and autumn values are below 5%, with some energetic peaks being expected for the northern sector, where wind speeds higher than 10 m/s may occur.

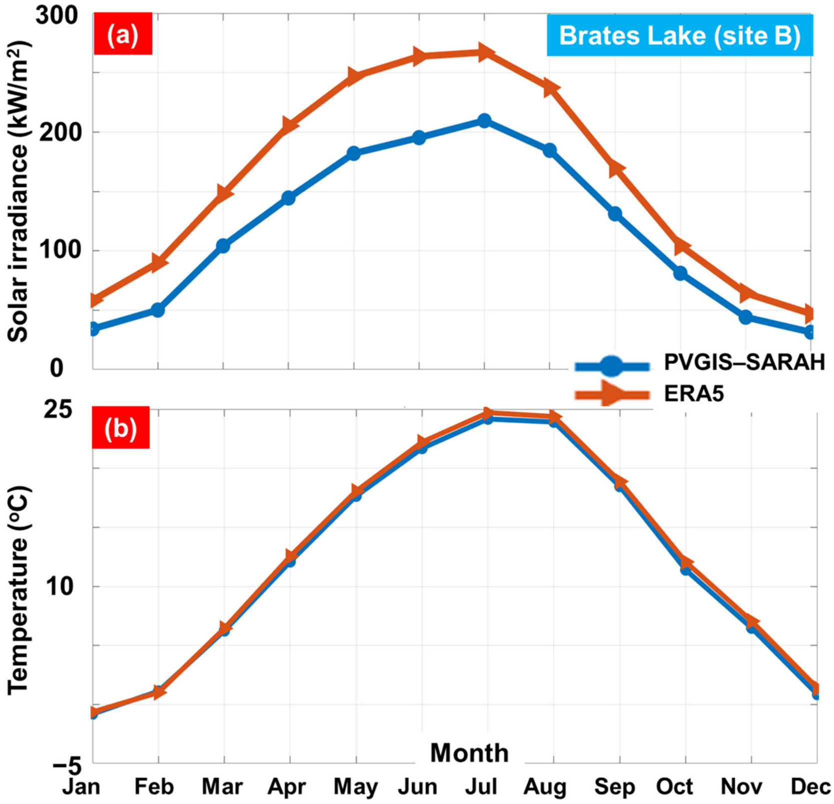

Figure 6. Brates Lake—monthly evolution of the solar irradiance (**a**) and temperature (**b**) associated with the SARAH and ERA5 datasets (average values), considering the time interval from 2005 to 2016.

The IEC 61400 (International Electrotechnical Commission) establishes in detail the requirements for the development and operation of a particular wind project. Among various parameters, this includes the IEC wind classes (from 1 to 4), that are defined by specific annual average wind speed values, namely [50], C1 (high wind)—10 m/s; C2 (medium wind)—8.5 m/s; C3 (low wind)—7.5 m/s; C4 (very low wind)—6 m/s. In Figure 8, the monthly distribution of these classes is highlighted, with the fact that in their selection, only the average wind speed was considered, without including additional details, such as the turbulence intensity or the 50 year gust events. As it is noticed, a site with values in class C1 will represent a suitable candidate for the development of a wind project. For the Brates Lake, these events are more frequent in January with maximum values of 6% (from monthly values). The values gradually increase as we move from C1 to C4, with a maximum of 9% being expected for class C2 (in March and December), 11% for class C3, or 22% for class C4 in February and March. These results were calculated based on the data associated with the thresholds indicated in the IEC guideline (mentioned above), which means that the missing values (up to 100%) are related to the *U*100 values located below 6 m/s. Based on these results, we can estimate that during the winter time, a particular wind turbine can obtain better performances compared to other time periods.

The solar energy potential can be indicated through the use of the solar irradiance (W/m^2), with the expectation that a site defined by average values of about 140 W/m^2 presents interest for the development of a photovoltaic project [51]. Figure 9 provides the annual distribution of the solar irradiance (average values), where the associated months were divided between each season. During the spring time (Figure 9a), better performances of an FPV system can be obtained in March with a maximum of 275 W/m^2 (in 2003), which is also possible that in some cases (for example, in 2020), April can become more important with a peak of 245 W/m^2. Moving to the summer season (Figure 9b), we can notice peaks of 294 W/m^2, but also significant inter-annual fluctuations that are in the range of [19.3–20.4]%. During the autumn time (Figure 9c), the values gradually decrease as we move to November, with an expected minimum value of 48.4 W/m^2. The values obtained are relatively constant, with some energetic peaks of 193 W/m^2 and 132 W/m^2 being noticed in September (2012) and October (2022), respectively. As it is noticed, during winter (Figure 9d), the values associated with December and January do not exceed 70 W/m^2, with higher values being expected from February that are in the range of (74.6–116) W/m^2.

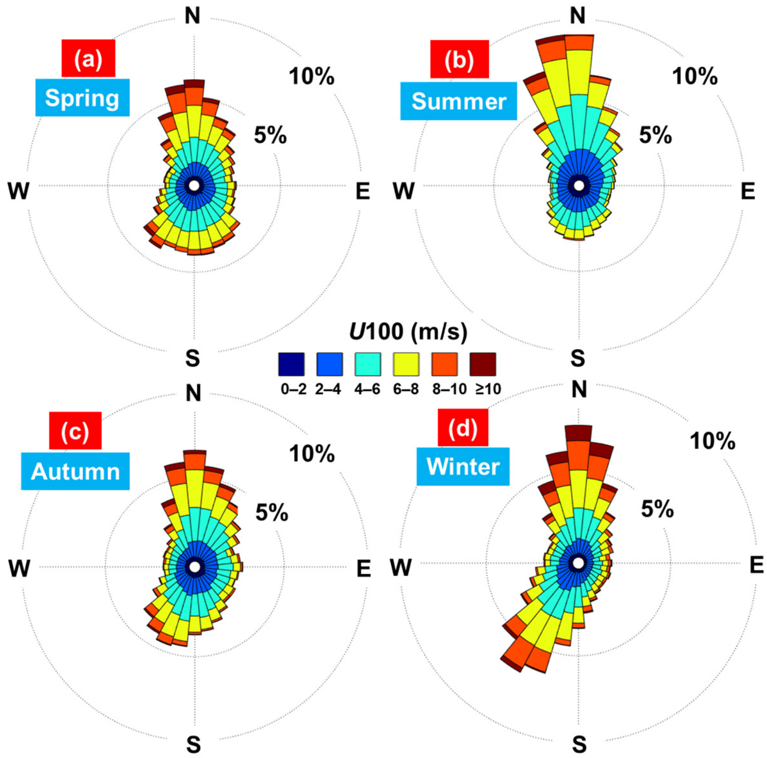

Figure 7. Wind roses associated with the Brates Lake (site B) considering the ERA5 dataset (2001–2022). The seasonal distributions of the *U*100 parameter are related to: (**a**) March–April–May; (**b**) June–July–August; (**c**) September–October–November; (**d**) December–January–February.

A more detailed analysis of the solar irradiance is highlighted in Figure 10, considering all the monthly/hourly combinations. A maximum peak of 725 W/m^2 is noticed during the interval June-August, while as expected, during the night solar power will not generate electricity. The time interval November-February is the less energetic one, with values that do not exceed 368 W/m^2. The summer time presents the best solar resources that can be classified into three intervals: (a) 06–07 AM and 04–05 PM—solar < 340 W/m^2; (b) 07–08 AM and 03–04 PM—solar < 490 W/m^2; (c) 08:00 AM–03:00 PM—solar irradiance between 490 and 725 W/m^2.

Besides the resource assessment, the present work aims to identify the expected performance of some solar and wind systems that may operate near the Brates Lake. A first analysis is provided in Figure 11, where the AEP of each wind turbine from Table 2 was estimated for different hub heights, as mentioned by the manufacturer. Although turbines T2 and T4 have the same rated capacity and relatively close operational hub heights, the AEP production is significantly influenced by the fact that turbine T4 has the lowest rated wind speed (11 m/s) from all the considered generators. Another drawback of turbine T2 is related to the higher value of the cut-in limit (4 m/s), which, for example, in the case of turbine T3, is associated with 2 m/s.

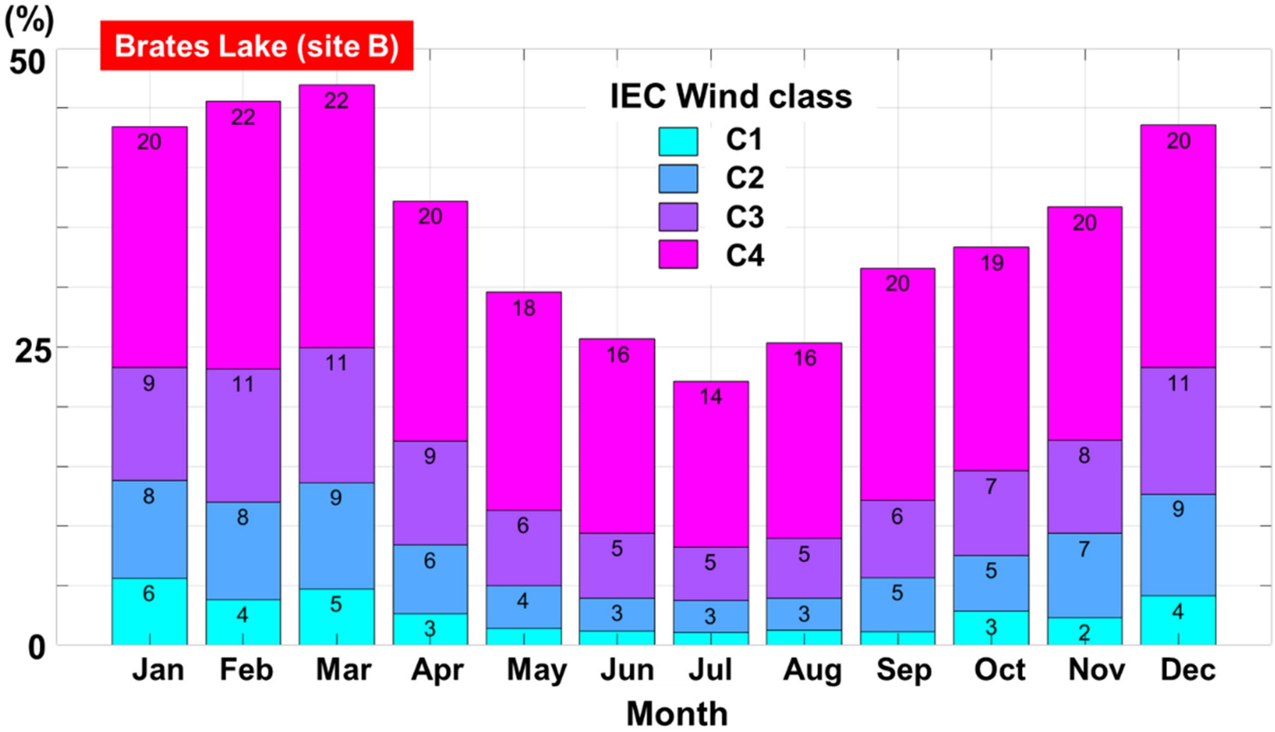

Figure 8. Monthly distribution of the IEC wind classes (ERA5 data) associated with site B. The results are defined for the interval 2001–2022, with a hub height of 100 m.

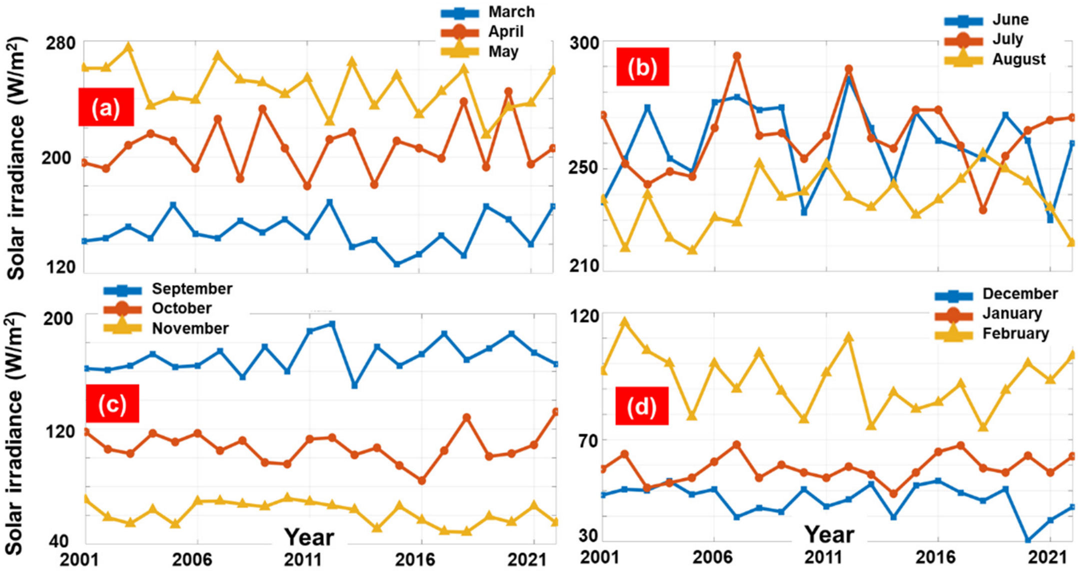

Figure 9. Brates Lake (site B)—solar irradiance (in W/m^2) corresponding to the ERA5 dataset, computed for the time interval 2001–2022. Average values associated with (**a**) spring; (**b**) summer; (**c**) autumn; (**d**) winter.

Although turbine T3 is defined by the highest hub height (138 m), such a solution is not justified, taking into account that a maximum AEP of 3.44 GWh can be obtained. This value is relatively close to the one expected from turbine T4, that may operate on a much lower hub height (for example, 67 m). The AEP production of these systems operates in the range of T1—2.61 and 2.78 GWh; T2—2.05 and 2.19 GWh; T3—3.12 and 3.44 GWh; T4—3.44 and 3.72 GWh.

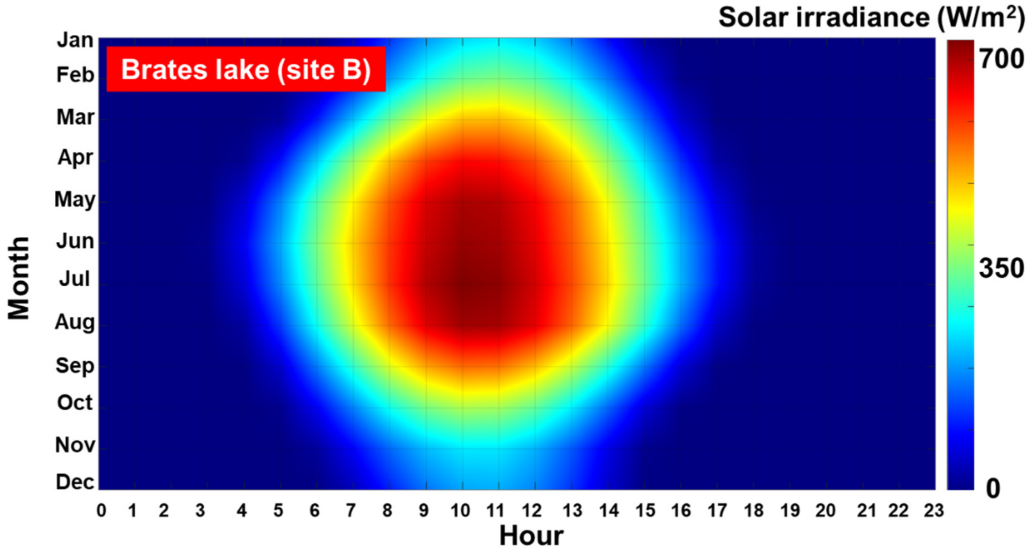

Figure 10. Brates Lake—distribution of the solar irradiance by months and hours, according to the average values of the ERA5 dataset (interval 2001–2022).

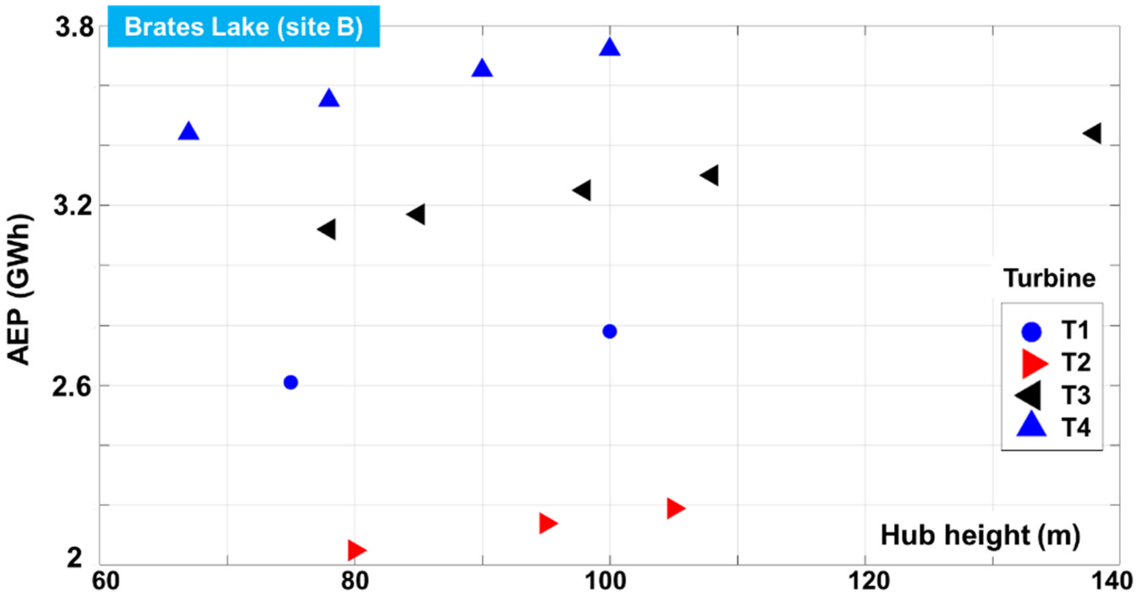

Figure 11. Brates Lake—AEP performance of the wind turbine considered, based on the ERA5 data (for the time interval 2001–2022). Results are processed for different hub heights.

Besides the AEP production, one way to identify the efficiency of a particular wind turbine is through the capacity factor (in %), that is the ratio between the average AEP production and the rated AEP production if a wind turbine will operate under optimal wind conditions [52]. In Table 5, such an analysis is presented, from which we can notice that turbine T4 is the only one that exceeds 21%, reaching a maximum of 21.23%. On the contrary, we may find that turbine T2 with a hub height of 80 m may expect a minimum capacity factor of 11.71%. Turbine T3 presents values in the range of 17.82 and 19.61%, compared to turbine T1, where a maximum value of 12.68% can be achieved. The present results are in line with the average capacity factor mentioned for some other onshore European areas [53,54], indicating values in the range of 20 and 30%.

Table 5. Capacity factor (%) of the wind turbines expected for the Brates Lake area. Results are based on ERA5 data (2001–2022), considering different hub heights.

Turbine	Hub Height (m)											
	67	**75**	**78**	**80**	**85**	**90**	**95**	**98**	**100**	**105**	**108**	**138**
T1		11.91							12.68			
T2				11.71			12.2			12.49		
T3			17.82		18.08			18.53			18.83	19.61
T4	19.64		20.24			20.81			21.23			

The onshore wind industry evolves very fast, including the occurrence of some large capacity generators. As a next step, in order to anticipate the implementations of a 6.2 MW wind turbine in the vicinity of Galati County, the performance of the Vestas V162-6.2 MW turbine was considered for evaluation, which was already implemented in some areas from Romania. From the official information provided by the Vestas producer, the rated wind speed value associated with this generator is missing, and for simplicity, two values (11 and 12 m/s) were assumed. This is in line with the trend from this sector, to lower the rated wind speed in order to obtain better performances [55]. In Figure 12, the performance of the Vestas V162-6.2 MW system is presented by considering all the possible scenarios (hub heights and rated wind speeds).

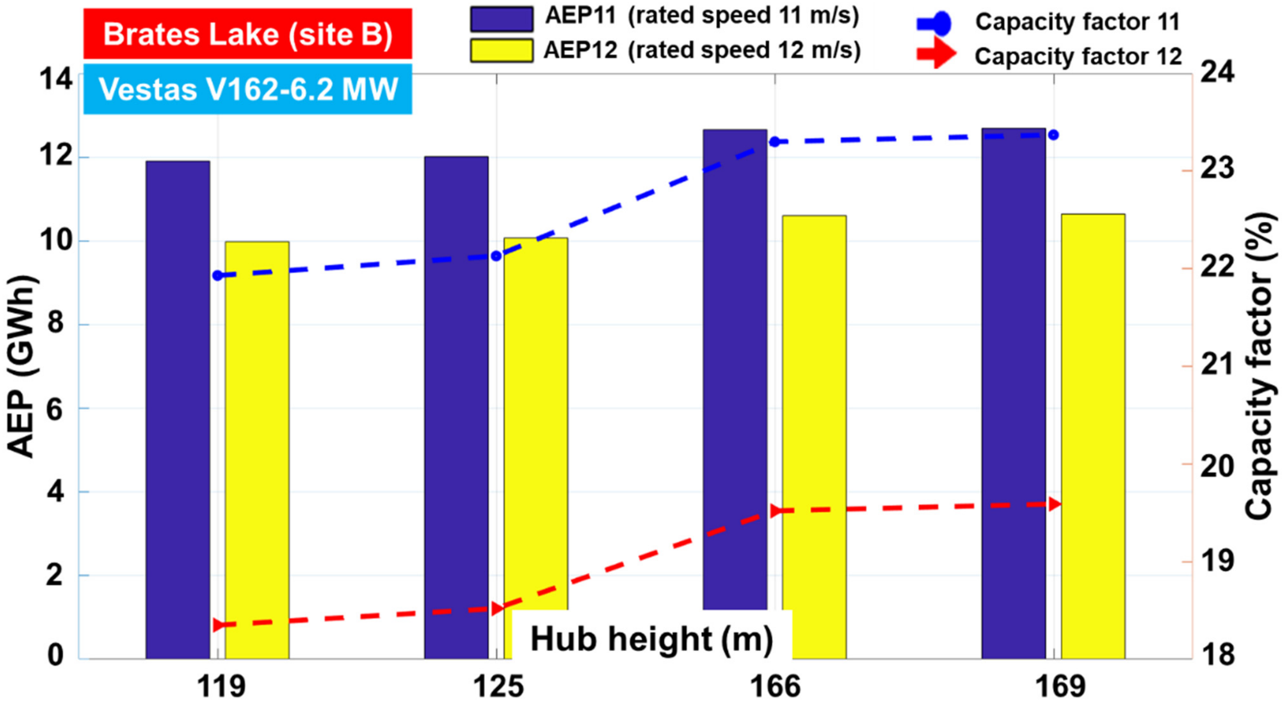

Figure 12. Performance of the Vestas V162-6.2 MW system expected from the Brates Lake location, according to the ERA5 data (for the time interval 2001–2022). The AEP and capacity factor are estimated for different hub heights and rated wind speeds (11 m/s and 12 m/s) of this generator.

As expected, better performances are associated with a rated speed of 11 m/s, with the AEP values ranging from 11.91 to 12.69 GWh according to the considered hub heights (from 119 to 169 m). For the same scenario, the capacity factor starts from 21.93% and reaches a maximum of 23.3% for hub heights, exceeding 166 m. For a wind turbine operating at a rated speed of 12 m/s, the performances decrease by 16.3% in the case of the AEP and capacity factor.

The idea of using a floating photovoltaic system is not new, as this was previously considered for different water bodies from Spain [45], Africa [56], Brazil [57], and even

Romania [46]. Looking at the existing literature, it was noticed that for a large water body, a floating project could cover almost 40% from the available area [58], and as a consequence, this limit was considered in the present work. In Figure 13, the AEP production of the four solar panels is indicated, and Table 3 presents the covered water area by the FPV systems, which gradually increased from 10% to 40%.

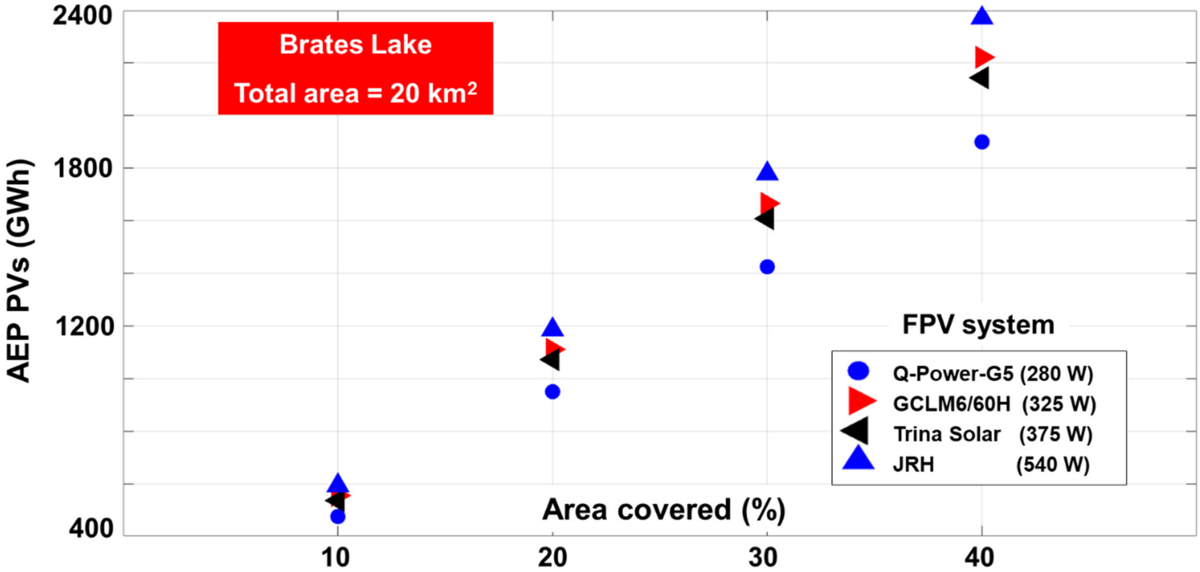

Figure 13. AEP performance of different floating PV modules operating on the Brates Lake. The results are based on ERA5 data (2001–2022), where the lake surface considered gradually increased from 10% to 40%, respectively.

The AEP production gradually increases with the covered area, starting from a minimum of 475 GWh in the case of P1 solar panel (10% area) and reaching a maximum of 2372 GWh for the system P4 (40% area) that is also defined by the highest capacity production of a single unit (540 W). This kind of project could provide, on an annual scale, the following average electricity output: (a) 10%—475 to 593 GWh (from P1 to P4); (b) 20%—950 to 1186 GWh; (c) 30%—1425 to 1779 GWh; (d) 40%—1900 to 2372 GWh. A 40% scenario (8 km^2) is difficult to obtain, although similar works propose scenarios involving water areas that exceed 20 km^2, from which 7434 GWh of solar electricity can be obtained [59].

Besides the electricity production, another objective of the present work is related to the impact of an FPV project on the Brates Lake water evaporation. Figure 14 presents such an analysis, where the natural evaporation from this area (no FPV) was estimated based on the ERA5 data and Equation (6). On an annual scale (Figure 14a), there are significant fluctuations, with minimum values of 1.02×10^7 m^3 and peaks of 1.36×10^7 m^3 being expected during the warmer years (for example, in 2017). In terms of the monthly projection (Figure 14b), during June and July, it is possible to reach a peak evaporation of 4.37×10^7 m^3, compared to only 0.43×10^7 m^3 which is expected for the winter period.

In Figure 15, the expected water volume saved by the presence of an FPV project that may operate on the Brates Lake is provided, considering the annual distribution. According to these results, the values range from a minimum of 0.5×10^6 m^3 in the case of the 10% scenario and reach up to a maximum of 3.27×10^6 m^3 for the 40% scenario.

A similar analysis was carried out in Figure 16, considering this time the monthly distribution. A scenario involving a 10% FPV farm may reduce the water evaporation with values in the range of [0.25–2.62] $\times 10^6$ m^3, gradually increasing to a maximum of 5.24×10^6 m^3 (for 20%), and 7.87 and 10.49×10^6 m^3 for the 30 and 40% scenarios.

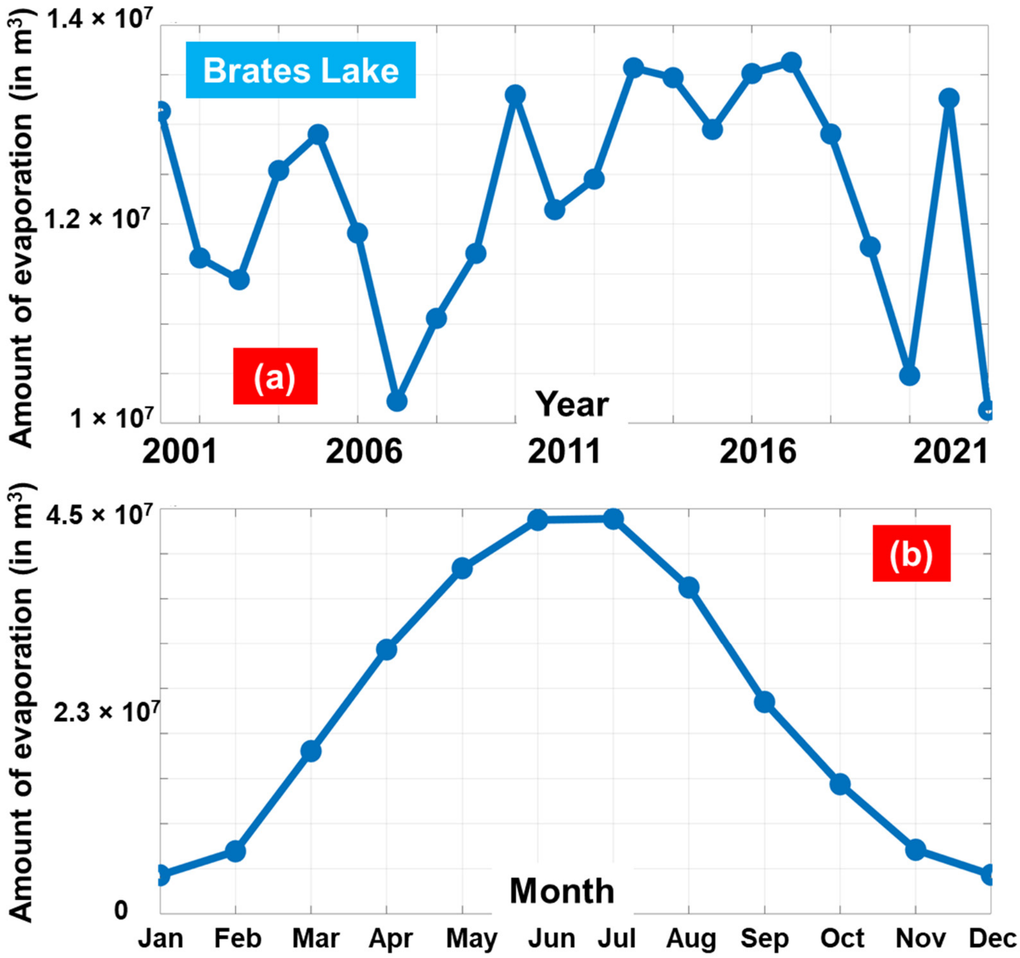

Figure 14. Water evaporation (in m^3) estimated for the entire Brates Lake area based on the ERA5 dataset (2001–2022), where: (**a**) annual variations; (**b**) monthly variations.

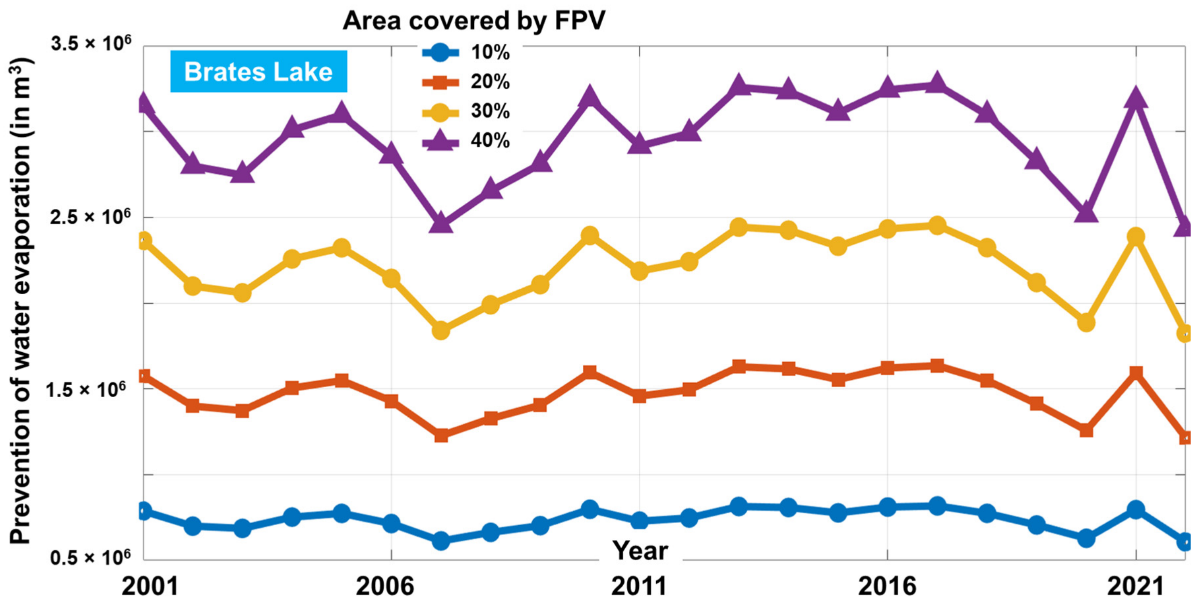

Figure 15. Annual water prevention from the implementation of FPV project, by considering different scenarios involving the Brates Lake (10, 20, 30, and 40%).

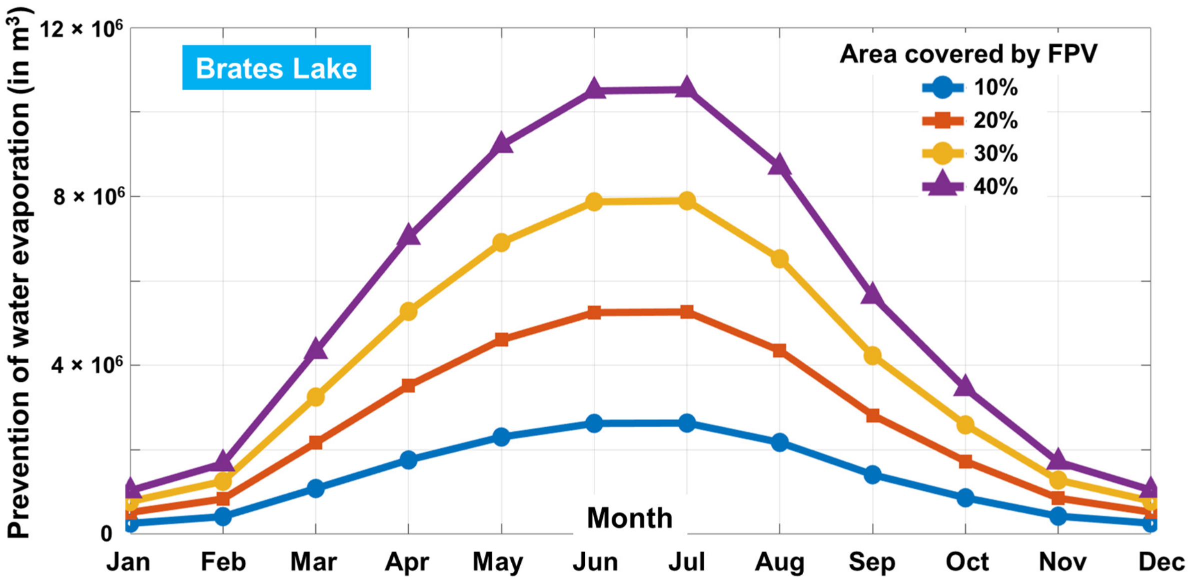

Figure 16. Monthly water prevention from the implementation of FPV project, by considering different scenarios involving the Brates Lake (10, 20, 30, and 40%).

The water scarcity represents a real issue, especially in the case of the agricultural sector. It is estimated that it is necessary to use an average water volume between 209 and 480 m^3, in order to obtain one ton of grain [60]. In some other works, it is suggested that for a single hectare (= 0.01 km^2) of agricultural land, an average of 0.394×10^8 m^3 of water consumption is required in order to run a successful project [61]. By comparing this number with the expected water volume saved by an FPV farm operating in the Brates Lake area, we can notice that even a 10% scenario can provide enough water for 3.42 km^2 of agricultural cultures, a value that increases to 13.71 km^2 in the case of a 40% scenario.

4. Conclusions

Although the north-eastern part of Romania is defined by attractive solar and wind resources that can be successfully used through a renewable project, there is little information in the public domain regarding the performances of this sector. Galati County has the potential to become a regional hot spot in terms of renewable sources, with the development of a wind project that will exceed the Fantanele–Cogealac capacity being expected in the near future, which is located in the vicinity of this area and is among the largest operational onshore wind parks in Europe. In addition, the Liberty Galati steel factory plans to implement an important hydrogen factory that will reduce the CO_2 emissions by almost 80%.

Based on the ERA5 data and on some in situ measurements, the dynamics of the wind and solar resources in the vicinity of the Brates Lake were evaluated, including the evolution of some other key parameters (temperature and evaporation). Although this lake is in an advanced degradation state, it still remains as one of the important water bodies from Romania. The ERA5 data for this area replicate quite well the monthly fluctuations of the average wind speed ($U10$), while significant differences occur when we discuss the maximum values.

From the performances of the renewable systems, we clearly highlight the AEP output of the Vestas V162-6.2 MW system that is expected to be installed in this region. One objective of the REPowerEU plan [61] is to implement several floating PVs in the marine environment or inland waters, in order to increase the electricity production, or eventually to reduce the water evaporation. In this context, the surface area of the Brates Lake (20 km^2) was considered to be gradually covered by solar panels, with the percentages varying from 10 to 40%. Besides the electricity output, it was found that if only 10% of this area could be covered, it would be possible to provide enough fresh water for almost 3.5 km^2 of agricultural land.

Finally, it is worth mentioning that this work is ongoing and some further research directions need to be considered. First, it will be important to implement a long-term monitoring station on the Brates Lake area, where various physical–chemical parameters of this lake will be recorded. In this way, it will be possible to check the accuracy of the present results, taking into account that they are mainly based on the ERA5 reanalysis data. In the case of the FPV systems, a general evaluation was carried out in terms of the electricity output, which may be considered a limitation of the present work. A more in-depth analysis is required, in order to properly identify the expected performances of various systems, where the layout of the panels or the optimal tilt angle will be properly taken into account. Another aspect may be related to the expected support that an inland FPV/wind project may provide for irrigation purposes and which solution will be more feasible from a technical and economic point of view.

Author Contributions: Writing—review and editing, E.R.; supervision and funding acquisition, P.L.G.; investigation, data processing, and visualization, F.O.; writing—original draft preparation, V.Y.; verification and interpretation of numerical results, S.D. All authors have read and agreed to the published version of the manuscript.

Funding: Technical support was provided by the Rexdan Research Infrastructure, the infrastructure created through the project An Integrated System for the Complex Environmental Research and Monitoring in the Danube River Area, REXDAN, SMIS code 127065, project co-financed by the European Regional Development Fund through the Competitiveness Operational Programme 2014–2020, contract no. 309/10.07.2020.

Data Availability Statement: No new data were created or analyzed in this study. Data sharing is not applicable to this article.

Acknowledgments: The ERA5 data used in this study were obtained from the Copernicus Climate Change Service (C3S), which is operated by the European Centre for Medium-Range Weather Forecasts (ECMWF). The in situ measurements were kindly provided by the National Meteorological Administration of Romania (NMA-RO).

Conflicts of Interest: S.D. is an employee of EnviroEcoSmart. Other authors declare no conflict of interest.

References

1. Wang, J.; Mamkhezri, J.; Khezri, M.; Karimi, M.S.; Khan, Y.A. Insights from European Nations on the Spatial Impacts of Renewable Energy Sources on CO_2 Emissions. *Energy Rep.* **2022**, *8*, 5620–5630. [CrossRef]
2. Durakovic, G.; del Granado, P.C.; Tomasgard, A. Powering Europe with North Sea Offshore Wind: The Impact of Hydrogen Investments on Grid Infrastructure and Power Prices. *Energy* **2023**, *263*, 125654. [CrossRef]
3. Wind Energy in Europe: 2022 Statistics and the Outlook for 2023–2027. Available online: https://windeurope.org/data-and-analysis/product/wind-energy-in-europe-2022-statistics-and-the-outlook-for-2023-2027 (accessed on 20 March 2023).
4. Madsen, D.N.; Hansen, J.P. Outlook of Solar Energy in Europe Based on Economic Growth Characteristics. *Renew. Sustain. Energy Rev.* **2019**, *114*, 109306. [CrossRef]
5. Kakoulaki, G.; Gonzalez Sanchez, R.; Gracia Amillo, A.; Szabo, S.; De Felice, M.; Farinosi, F.; De Felice, L.; Bisselink, B.; Seliger, R.; Kougias, I.; et al. Benefits of Pairing Floating Solar Photovoltaics with Hydropower Reservoirs in Europe. *Renew. Sustain. Energy Rev.* **2023**, *171*, 112989. [CrossRef]
6. Agrawal, K.K.; Jha, S.K.; Mittal, R.K.; Vashishtha, S. Assessment of Floating Solar PV (FSPV) Potential and Water Conservation: Case Study on Rajghat Dam in Uttar Pradesh, India. *Energy Sustain. Dev.* **2022**, *66*, 287–295. [CrossRef]
7. Mamatha, G.; Kulkarni, P.S. Assessment of Floating Solar Photovoltaic Potential in India's Existing Hydropower Reservoirs. *Energy Sustain. Dev.* **2022**, *69*, 64–76. [CrossRef]
8. Zuzana, D. Where Sun Meets Water: Floating Solar Handbook for Practitioners. Available online: https://documents.worldbank.org/pt/publication/documents-reports/documentdetail/418961572293438109/Where-Sun-Meets-Water-Floating-Solar-Handbook-for-Practitioners (accessed on 20 March 2023).
9. Cebotari, S.; Cristea, M.; Moldovan, C.; Zubascu, F. Renewable Energy's Impact on Rural Development in Northwestern Romania. *Energy Sustain. Dev.* **2017**, *37*, 110–123. [CrossRef]

10. Ionescu, R.V.; Antohi, V.M.; Zlati, M.L.; Georgescu, L.P.; Iticescu, C. To a Green Economy across the European Union. *Int. J. Environ. Res. Public Health* **2022**, *19*, 12427. [CrossRef]
11. Vrînceanu, A.; Dumitrașcu, M.; Kucsicsa, G. Site Suitability for Photovoltaic Farms and Current Investment in Romania. *Renew. Energy* **2022**, *187*, 320–330. [CrossRef]
12. Onea, F.; Ciortan, S.; Rusu, E. Assessment of the Potential for Developing Combined Wind-Wave Projects in the European Nearshore. *Energy Environ.* **2017**, *28*, 580–597. [CrossRef]
13. Dragomir, G.; Șerban, A.; Năstase, G.; Brezeanu, A.I. Wind Energy in Romania: A Review from 2009 to 2016. *Renew. Sustain. Energy Rev.* **2016**, *64*, 129–143. [CrossRef]
14. Onea, F.; Rusu, L. A Study on the Wind Energy Potential in the Romanian Coastal Environment. *J. Mar. Sci. Eng.* **2019**, *7*, 142. [CrossRef]
15. Răileanu, A.B.; Rusu, L.; Rusu, E. An Evaluation of the Dynamics of Some Meteorological and Hydrological Processes along the Lower Danube. *Sustainability* **2023**, *15*, 6087. [CrossRef]
16. Business Romania. Latest News from Business in Romania Only at ZF English. Available online: https://www.zfenglish.com/ (accessed on 21 March 2023).
17. LIBERTY Galati GREENSTEEL Transformation Plan. Available online: https://libertysteelgroup.com/delivering_cn30/liberty-galati-greensteel-transformation-plan/ (accessed on 22 March 2023).
18. Constantin, D.-E.; Bocăneala, C.; Voiculescu, M.; Roşu, A.; Merlaud, A.; Roozendael, M.V.; Georgescu, P.L. Evolution of SO_2 and NOx Emissions from Several Large Combustion Plants in Europe during 2005–2015. *Int. J. Environ. Res. Public Health* **2020**, *17*, 3630. [CrossRef] [PubMed]
19. Popa, P.; Murariu, G.; Timofti, M.; Georgescu, L.P. Multivariate Statistical Analyses of Danube River Water Quality at Galati, Romania. *Environ. Eng. Manag. J.* **2018**, *17*, 1249–1266. [CrossRef]
20. Ţuţuianu, L.; Vespremeanu-Stroe, A.; Preoteasa, L.; Rotaru, S.; Dima, A.; Dimofte, D. Wetlands and Lakes Formation and Evolution on the Lower Danube Floodplain during Middle and Late Holocene. *Quat. Int.* **2021**, *602*, 82–91. [CrossRef]
21. Avram, S.; Cipu, C.; Corpade, A.-M.; Gheorghe, C.A.; Manta, N.; Niculae, M.-I.; Pascu, I.S.; Szép, R.E.; Rodino, S. GIS-Based Multi-Criteria Analysis Method for Assessment of Lake Ecosystems Degradation—Case Study in Romania. *Int. J. Environ. Res. Public Health* **2021**, *18*, 5915. [CrossRef]
22. Banescu, A.; Arseni, M.; Georgescu, L.P.; Rusu, E.; Iticescu, C. Evaluation of Different Simulation Methods for Analyzing Flood Scenarios in the Danube Delta. *Appl. Sci.* **2020**, *10*, 8327. [CrossRef]
23. Ion, I.M.D.; Dincă, C.S.; Șerban, C.B.; Stanciu, S. Agricultural Sector in Galaţi County. Resources for the Seed Production. In Proceedings of the 31st International Business Information Management Association Conference, Milan, Italy, 25–26 April 2018; International Business Information Management Association (IBIMA): King of Prussia, PA, USA, 2018.
24. Calmuc, M.; Calmuc, V.; Arseni, M.; Topa, C.; Timofti, M.; Georgescu, L.P.; Iticescu, C. A Comparative Approach to a Series of Physico-Chemical Quality Indices Used in Assessing Water Quality in the Lower Danube. *Water* **2020**, *12*, 3239. [CrossRef]
25. Apetrei, C.; Iticescu, C.; Georgescu, L.P. Multisensory System Used for the Analysis of the Water in the Lower Area of River Danube. *Nanomaterials* **2019**, *9*, 891. [CrossRef]
26. Calmuc, V.A.; Calmuc, M.; Arseni, M.; Topa, C.M.; Timofti, M.; Burada, A.; Iticescu, C.; Georgescu, L.P. Assessment of Heavy Metal Pollution Levels in Sediments and of Ecological Risk by Quality Indices, Applying a Case Study: The Lower Danube River, Romania. *Water* **2021**, *13*, 1801. [CrossRef]
27. Guillory, A. ERA5. Available online: https://www.ecmwf.int/en/forecasts/datasets/reanalysis-datasets/era5 (accessed on 31 May 2019).
28. Soukissian, T.H.; Karathanasi, F.E.; Zaragkas, D.K. Exploiting Offshore Wind and Solar Resources in the Mediterranean Using ERA5 Reanalysis Data. *Energy Convers. Manag.* **2021**, *237*, 114092. [CrossRef]
29. Jurasz, J.; Mikulik, J.; Dąbek, P.B.; Guezgouz, M.; Kaźmierczak, B. Complementarity and 'Resource Droughts' of Solar and Wind Energy in Poland: An ERA5-Based Analysis. *Energies* **2021**, *14*, 1118. [CrossRef]
30. Bouallègue, Z.B.; Cooper, F.; Chantry, M.; Düben, P.; Bechtold, P.; Sandu, I. Statistical Modeling of 2-m Temperature and 10-m Wind Speed Forecast Errors. *Mon. Weather. Rev.* **2023**, *151*, 897–911. [CrossRef]
31. Archer, C.L.; Jacobson, M.Z. Evaluation of Global Wind Power. *J. Geophys. Res. Atmos.* **2005**, *110*, 1–20. [CrossRef]
32. Liu, B.; Ma, X.; Guo, J.; Li, H.; Jin, S.; Ma, Y.; Gong, W. Estimating Hub-Height Wind Speed Based on a Machine Learning Algorithm: Implications for Wind Energy Assessment. *Atmos. Chem. Phys.* **2023**, *23*, 3181–3193. [CrossRef]
33. de Souza Nascimento, M.M.; Shadman, M.; Silva, C.; de Freitas Assad, L.P.; Estefen, S.F.; Landau, L. Offshore Wind and Solar Complementarity in Brazil: A Theoretical and Technical Potential Assessment. *Energy Convers. Manag.* **2022**, *270*, 116194. [CrossRef]
34. Khalifeh Soltani, S.R.; Mostafaeipour, A.; Almutairi, K.; Hosseini Dehshiri, S.J.; Hosseini Dehshiri, S.S.; Techato, K. Predicting Effect of Floating Photovoltaic Power Plant on Water Loss through Surface Evaporation for Wastewater Pond Using Artificial Intelligence: A Case Study. *Sustain. Energy Technol. Assess.* **2022**, *50*, 101849. [CrossRef]
35. Hayibo, K.S.; Pearce, J.M. Foam-Based Floatovoltaics: A Potential Solution to Disappearing Terminal Natural Lakes. *Renew. Energy* **2022**, *188*, 859–872. [CrossRef]

36. Mittal, D.; Kumar Saxena, B.; Rao, K.V.S. Potential of Floating Photovoltaic System for Energy Generation and Reduction of Water Evaporation at Four Different Lakes in Rajasthan. In Proceedings of the 2017 International Conference on Smart Technologies For Smart Nation (SmartTechCon), Bengaluru, India, 17–19 August 2017; IEEE: Piscataway, NJ, USA, 2017; pp. 238–243.
37. Urraca, R.; Gracia-Amillo, A.M.; Koubli, E.; Huld, T.; Trentmann, J.; Riihelä, A.; Lindfors, A.V.; Palmer, D.; Gottschalg, R.; Antonanzas-Torres, F. Extensive Validation of CM SAF Surface Radiation Products over Europe. *Remote Sens. Environ.* **2017**, *199*, 171–186. [CrossRef]
38. Riihelä, A.; Kallio, V.; Devraj, S.; Sharma, A.; Lindfors, A.V. Validation of the SARAH-E Satellite-Based Surface Solar Radiation Estimates over India. *Remote Sens.* **2018**, *10*, 392. [CrossRef]
39. V162-6.2 MWTM. Available online: https://www.vestas.com/en/products/enventus-platform/v162-6-2-mw (accessed on 16 May 2023).
40. Welcome to Wind-Turbine-Models.Com. Available online: https://en.wind-turbine-models.com/ (accessed on 20 May 2018).
41. Wind Energy Database. Available online: https://www.thewindpower.net/index.php (accessed on 1 May 2019).
42. Rusu, E. An Evaluation of the Wind Energy Dynamics in the Baltic Sea, Past and Future Projections. *Renew. Energy* **2020**, *160*, 350–362. [CrossRef]
43. Rusu, E.; Onea, F. A Parallel Evaluation of the Wind and Wave Energy Resources along the Latin American and European Coastal Environments. *Renew. Energy* **2019**, *143*, 1594–1607. [CrossRef]
44. López, M.; Rodríguez, N.; Iglesias, G. Combined Floating Offshore Wind and Solar PV. *J. Mar. Sci. Eng.* **2020**, *8*, 576. [CrossRef]
45. López, M.; Soto, F.; Hernández, Z.A. Assessment of the Potential of Floating Solar Photovoltaic Panels in Bodies of Water in Mainland Spain. *J. Clean. Prod.* **2022**, *340*, 130752. [CrossRef]
46. Manolache, A.I.; Andrei, G.; Rusu, L. An Evaluation of the Efficiency of the Floating Solar Panels in the Western Black Sea and the Razim-Sinoe Lagunar System. *J. Mar. Sci. Eng.* **2023**, *11*, 203. [CrossRef]
47. Maraj, A.; Kërtusha, X.; Lushnjari, A. Energy Performance Evaluation for a Floating Photovoltaic System Located on the Reservoir of a Hydro Power Plant under the Mediterranean Climate Conditions during a Sunny Day and a Cloudy-One. *Energy Convers. Manag. X* **2022**, *16*, 100275. [CrossRef]
48. Fereshtehpour, M.; Javidi Sabbaghian, R.; Farrokhi, A.; Jovein, E.B.; Ebrahimi Sarindizaj, E. Evaluation of Factors Governing the Use of Floating Solar System: A Study on Iran's Important Water Infrastructures. *Renew. Energy* **2021**, *171*, 1171–1187. [CrossRef]
49. Hersbach, H.; Bell, B.; Berrisford, P.; Hirahara, S.; Horányi, A.; Muñoz-Sabater, J.; Nicolas, J.; Peubey, C.; Radu, R.; Schepers, D.; et al. The ERA5 Global Reanalysis. *Q. J. R. Meteorol. Soc.* **2020**, *146*, 1999–2049. [CrossRef]
50. Wang, H.; Blaabjerg, F.; Ma, K.; Wu, R. Design for Reliability in Power Electronics in Renewable Energy Systems–Status and Future. In Proceedings of the 4th International Conference on Power Engineering, Energy and Electrical Drives, Istanbul, Turkey, 13–17 May 2013; IEEE: Piscataway, NJ, USA, 2013; pp. 1846–1851.
51. Abed, K.A.; El-Mallah, A.A. Capacity Factor of Wind Turbines. *Energy* **1997**, *22*, 487–491. [CrossRef]
52. Michalco, B.T. Kim Tranberg and David Statistics. Available online: https://turbines.dk/statistics (accessed on 3 April 2023).
53. Staffell, I.; Green, R. How Does Wind Farm Performance Decline with Age? *Renew. Energy* **2014**, *66*, 775–786. [CrossRef]
54. Boretti, A.; Castelletto, S. Trends in Performance Factors of Wind Energy Facilities. *SN Appl. Sci.* **2020**, *2*, 1718. [CrossRef]
55. Gonzalez Sanchez, R.; Kougias, I.; Moner-Girona, M.; Fahl, F.; Jäger-Waldau, A. Assessment of Floating Solar Photovoltaics Potential in Existing Hydropower Reservoirs in Africa. *Renew. Energy* **2021**, *169*, 687–699. [CrossRef]
56. Padilha Campos Lopes, M.; Nogueira, T.; Santos, A.J.L.; Castelo Branco, D.; Pouran, H. Technical Potential of Floating Photovoltaic Systems on Artificial Water Bodies in Brazil. *Renewable Energy* **2022**, *181*, 1023–1033. [CrossRef]
57. Resources.Solarbusinesshub.com. Floating Solar Photovoltaic (FSPV): A Third Pillar to Solar PV Sector? Available online: https://resources.solarbusinesshub.com/solar-industry-reports/item/floating-solar-photovoltaic-fspv-a-third-pillar-to-solar-pv-sector (accessed on 4 April 2023).
58. Pouran, H.; Padilha Campos Lopes, M.; Ziar, H.; Alves Castelo Branco, D.; Sheng, Y. Evaluating Floating Photovoltaics (FPVs) Potential in Providing Clean Energy and Supporting Agricultural Growth in Vietnam. *Renew. Sustain. Energy Rev.* **2022**, *169*, 112925. [CrossRef]
59. Wang, Z.; Nguyen, T.; Westerhoff, P. Food–Energy–Water Analysis at Spatial Scales for Districts in the Yangtze River Basin (China). *Environ. Eng. Sci.* **2019**, *36*, 789–797. [CrossRef]
60. Bao, Q.; Ding, J.; Han, L.; Li, J.; Ge, X. Predicting Land Change Trends and Water Consumption in Typical Arid Regions Using Multi-Models and Multiple Perspectives. *Ecol. Indic.* **2022**, *141*, 109110. [CrossRef]
61. Vezzoni, R. Green Growth for Whom, How and Why? The REPowerEU Plan and the Inconsistencies of European Union Energy Policy. *Energy Res. Soc. Sci.* **2023**, *101*, 103134. [CrossRef]